2021 7th International Conference on Hydraulic and Civil Engineering & Smart Water Conservancy and Intelligent Disaster Reduction Forum (ICHCE & SWIDR)

Numerical Analysis of the Influence of Tunnel Excavation on the Changes of Surrounding Rock Stress and Displacement

Libo Ding[1], Xing Chen[2], Youchuan Wu[3*] and Xiaopeng Wang[3]
[1] China Road and Bridge Engineering Co., Ltd., Beijing, China
[2] CCCC Second Highway Engineering Co., Ltd., Xi'an, China
[3] Xi'an University of Architecture and Technology, Xi'an, China
*Corresponding author's e-mail: xauatwyc@163.com

Abstract. **The Argveta exit of No. 2 Tunnel in Georgia is taken as the research object, and the three-dimensional geological numerical analysis model of the tunnel is established. The model simulates the construction condition of full-section tunnel excavation through passivation, and discusses the variation law of stress and displacement caused by excavation. According to the study results, with the construction of the tunnel, the surrounding rock pressure increases gradually, which has a lot to do with the tunnel excavation footage and temporary support time; the deformation of tunnel entrance is greatly affected by tunnel excavation, which has a gradual Increasing trend; for the simultaneous construction of tunnels with different spans, the impact of the excavation of a large-span tunnel on the rock, soil, temporary lining and the secondary lining is greater than the stress and deformation of a small-span tunnel.**

Keywords-Numerical analysis; tunnel excavation; surrounding rock pressure; surrounding rock displaceme

I. Introduction

Nowadays, with the more and more mature computer technology, the application of tunnel numerical simulation has been quite extensive. In the process of numerical modeling, how to extract a reasonable boundary range from the actual project, balance the relationship between calculation accuracy and memory occupation, and select better combination points are crucial links in numerical modeling.

By using the numerical simulation, Song Zhanping[1-2] optimizes the construction scheme of large-section tunnel, Xu Qianwei[3] studies the failure process of surrounding rock during the construction of fault tunnel, Chen Lihan[4] analyzes the stress distribution of surrounding rock caused by various excavation methods, Xing Jun[5] studies the process of deformation and breakage of the surrounding rock under the condition of continuous rainfall and construction of the Songduo Tunnel, and Zhang Zhengliang[6] analyzes the surrounding rock deformation and the stress of the tunnel lining under the two sets of working conditions. Guo Zihong[7-8] analyzes the fracture surface distribution of shallow buried tunnel and proposes a stability evaluation method of shallow buried tunnel. According to the numerical simulation results, Liu Bo[9] proposes the control measures of tunnel deformation. Niu Yonghong[10] simulates various excavation methods of shallow buried tunnel by using finite element software. Li Kang[11] conducts a systematic and comprehensive on-site monitoring of the surrounding rock pressure and surrounding rock stratum displacement in Xinhua Tunnel.

This paper takes the proposed Georgia No.2 tunnel as the study object and builds a numerical model through MIDAS GTS NX. By simulating the full-face excavation to explore the displacement and stress transformation rule of surrounding rock, and some suggestions and references are given in the design and construction decision of tunnel.

II. Project Overview

The proposed tunnel is located between the central part of the Georgian block, the Transcaucasus block, the Greater Caucasus in the north and the Lesser Caucasus in the south. The starting and ending mileage is K3+122.500~K4+760.000, the designed total length is 1637.5m, the maximum value of depth is 277.3m and the minimum value is 251m. The clearance spans of the left and right tunnels are 9.6 and 11.6 m respectively, and the distance between them is 14.2m. The tunnel is excavated through the PzGr strata, which is composed of metamorphic and intrusive rocks of the Proterozoic crystalline basement. The surrounding rock grade is III~IV. Considering the complexity of the excavation process and the stability of the slope, a micro-pile wall of ϕ240.0 mm is used for support.

III. Tunnel Finite Element Model

According to the software's applicable conditions and material model for the lithology of the tunnel surrounding rock, this model uses the ideal elastic-plastic model and adapts the Moore-Coulomb criterion as the destruction condition.

A. Parameter selection

The proposed tunnel has complex lithology, so a simplified model (from K4+720 to K4+760) is established, there is no bad geological zone in this section. And this model ignores the influence of groundwater. The micro-pile wall and the temporary lining are made of C30 concrete, the second lining vault and invert are made of C35 and C30 concrete. Related parameters are given in Table 1.

978-1-6654-0865-3/21/$31.00 ©2021 IEEE

Table 1. Physical and Mechanical Parameters of Surrounding Rock and Lining Materials

Material name	Constitutive type	Unit type	E(kPa)	γ(kN/m^3)	μ	C(kPa)	φ(°)
Rock	Mohr-Coulomb	Physical unit	1.0 e^6	25	0.25	100	54
Concrete (tunnel entrance)	Elasticity	Physical unit	3.0e^7	24	0.20	-	-
Temporary Lining	Elasticity	Board unit	3.0e^7	24	0.20	-	-
Invert	Elasticity	Board unit	3.15e^7	25	0.20	-	-
Vault	Elasticity	Board unit	3.15e^7	25	0.2	-	-
pile	Elasticity	Implantable beam unit	2.8e^7	23	0.2	-	-

Note: γ = unit weight; c = cohesion; φ = friction angle; E = deformation modulus; μ = Poisson's ratio.

B. Model establishment

Excavation will cause stress redistribution, according to the numerical distribution of stress in excavation theory and practical experience, the distribution range is within 3 times the tunnel radius. The larger tunnel radius is 5.5m, so the distance between the bottom of the tunnel and the bottom of the model is 17.5m, the depth of the tunnel in the model is subject to the actual elevation data. The model size is 70m×40m. After the model is built, boundary constraints and self-weight are imposed on it. As shown in Figure 1, the left and front sides are fixed by horizontal constraints, and the lower side is fixed by a combination of horizontal and vertical constraints.

The model is divided into mixed grids and includes 48910 cells and 24858 nodes. Figure 2 gives the mesh of the three-dimensional model. The rock and soil, tunnel and portal sections are simulated by 3D solid elements, the temporary lining and secondary lining of the tunnel are simulated by 2D slab elements, and 1D implanted beams can simulate micro-pile walls. Because the proposed tunnel has large horizontal tectonic stress and strong historical tectonic activity, the lateral pressure coefficient is 1.0, and its initial stress field is established accordingly.

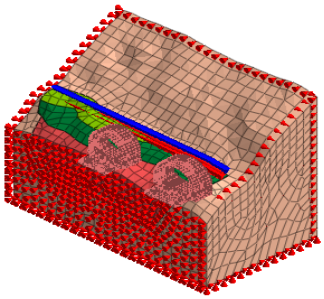

Figure 1. Boundary constraints of model

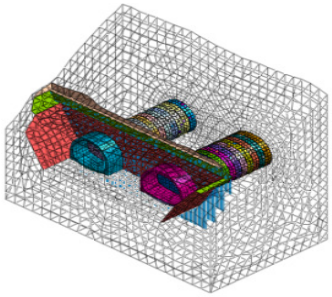

Figure 2. Model grid

IV. Finite element analysis of tunnel excavation

A. Construction conditions

The tunnel is constructed by full-section excavation, and its software implementation is mainly through the passivation or activation of the tunnel grid through the MIDAS GTS NX. The tunnel excavation includes 29 work steps. The first 6 steps are the preparation for the excavation of the tunnel, tunnel excavation is the seventh step. According to the type of tunnel section, the first excavation footage is 6m, then the tunnel is excavated with 2-meter footage. To avoid interfering with construction and causing some rock blocks to lose mutual support and become loose and wrong, the temporary lining should be constructed in time for a certain distance after the excavation. After the temporary lining is completed and the deformation is stabilized, the second lining is applied to the tunnel at the 19th step of simulated construction, to achieve the effect of reinforcement and support.

B. Simulation result analysis

When the tunnel is excavated, the natural stress of the surrounding rock is redistributed, and the secondary stress balance is reached after the support, forming a redistributed stress field. This article will analyse the stress and displacement of rock and soil, temporary lining, and secondary lining.

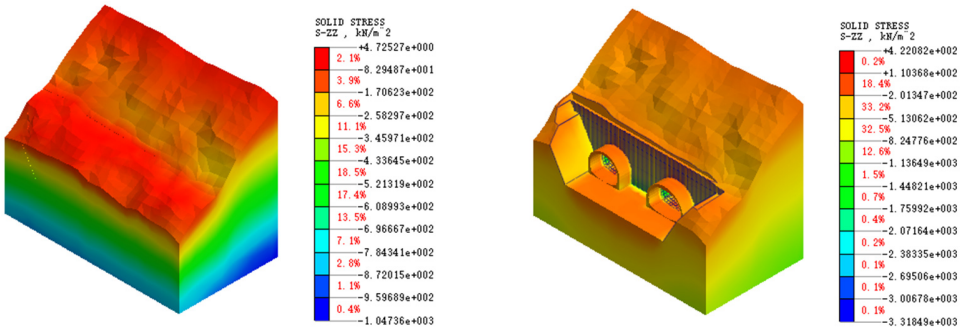

(a) The initial stage

(b) The end of excavation

Figure 3. Nephogram of Maximum Principal Stress Distribution of Surrounding Rock

1) Distribution of surrounding rock pressure. With the excavation of the tunnel, the surrounding rock pressure changes significantly, and the rock and soil mass changes from the natural stress state to the stress redistribution state. In this paper, the maximum principal stress at the initial stage and the end stage of tunnel excavation are analyzed. In Figure 3, the maximum principal stress changes from -1.047~+0.004Mpa at the initial stage to -3.318~0.422Mpa at the end of the tunnel excavation, the maximum value increases by 104.5 times and the minimum value increases by about 2 times. After excavation, the maximum and minimum maximum principal stresses vary from the surface and bottom of the rock mass to the invert and tunnel waist.

The stress of the surrounding rock in the vertical direction gradually increases, which has a lot to do with the length of the tunnel excavation and the temporary lining. In Figure 4, from the third step to the fourth step, a mass of rock and soil in the third layer are excavated, resulting in an increase in compressive stress, and the decline in the sixth step to the seventh step is due to the excavation of the rock and soil. This is because slope support is carried out in time, and the support structure withstands part of the surrounding rock stress. From the overall trend, the rock and soil are mainly compressed, the overall tensile stress does not change much, and the maximum value appears at the tunnel invert. The maximum value of compressive stress increases gradually, until the 18th construction step. When the construction of excavation and temporary support are finished, the maximum value of compressive stress occurs at the right tunnel arch waist, and the maximum principal stress basically tends to be stable.

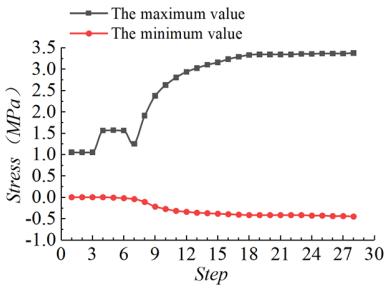

Figure 4. Stress Diagram of Vertical Surrounding Rock

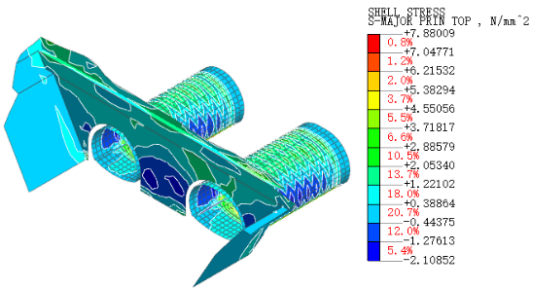

Figure 5. Isogram of Temporary Support Stress

2) Temporary support, stress distribution of the secondary lining. The excavation of the tunnel will disturb the rock mass, which will cause the loose rock mass to fall or the surrounding rock deforms greatly. Therefore, timely temporary support is necessary. In the simulation process of this paper, according to the excavation step followed by shotcrete as temporary support, which ensures sufficient clearance for tunnel construction, prevents rock deformation and withstands surrounding rock pressure. Figure 5 gives the temporary support stress cloud when the excavation is over.

As shown in Figure 6 and Figure 7, with the construction of the tunnel, the maximum principal stresses of the tunnel temporary lining and the second lining did not change significantly, which also shows that the rationality of the arrangement between excavation and support. Support the excavated tunnel in time to make it bear pressure, which will help maintain the surrounding rock stable.

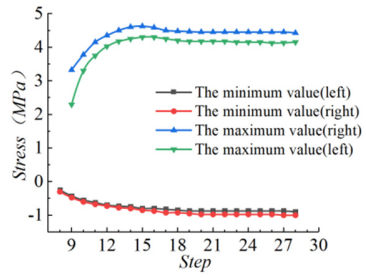

Figure 6. Maximum Principal Stress Diagram of Temporary Lining

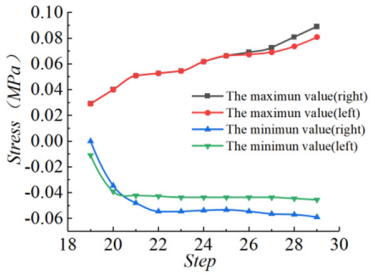

Figure 7. Maximum principal stress diagram of second lining

C. Tunnel displacement analysis

1) Analysis of Displacement of Tunnel Entrance Section. During the tunnel excavation, the displacement of the right tunnel is larger because its radius is larger. Figures 8 gives the maximum total displacement and vertical Directional displacement, the construction of the entrance is simulated in step 9. Throughout the excavation process, there is always a large displacement at the top of the inlet, the maximum displacement occurs at the top of the right inlet, approximately 14.13mm. The maximum uplift displacement caused by tunnel excavation is 6.412mm, which appears at the edge of the platform formed after the excavation of the rock and soil, and the maximum value of vertical settlement appears at the top of the right opening and is approximately 13.48mm.

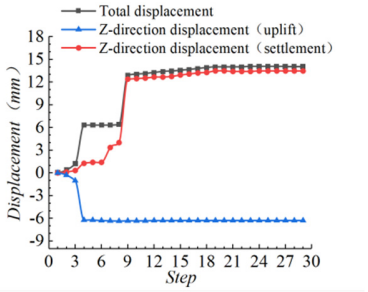

Figure 8. Diagram of vertical and total displacements caused by tunnel excavation (Note: The displacement caused by tunnel excavation is defined as "+" for settlement and "-" for uplift)

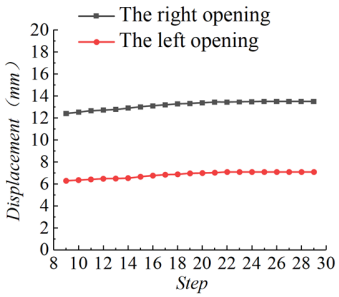

Figure 9. Displacement diagram of a joint in the vault of left and right openings

According to the large displacement of the entrance part, a node on the top of the left and right entrance is selected. It can be seen from Figure 9 that the displacement increases rapidly from step 8 to step 18 of construction. After the construction of the left opening is completed, the displacement increases from 6.24 mm in step 9 to 6.81 mm in step 18. The displacement curve of step 29 is relatively slow. The displacement increases from 6.95mm in step 19 to 7.06mm in step 29. The change law of the right and left openings is consistent, so we will not repeat them.

2) Analysis of the Lining Displacement. From the beginning of the temporary support in step 8 to the end of the temporary lining in step 18, the maximum displacement of the left and right tunnel temporary support vault and arch bottom are shown in Figure 10: the uplift of the left (right) tunnel arch bottom gradually decreases, which is due to the temporary support on the surrounding rock deformation limit. The settlement of tunnel vault increases at a steady rate. Because the tunnel section is asymmetric, the displacement of the temporary support in right tunnel is about 1mm larger than left tunnel. Different excavation sections have different influences on the support displacement.

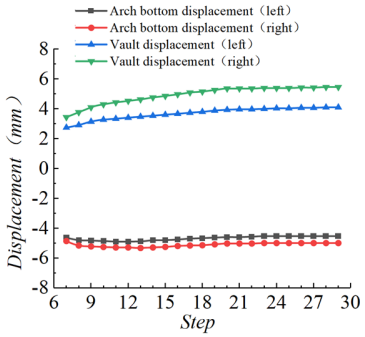

Figure 10. Displacement Diagram of Temporary Lining of Left and Right Tunnels

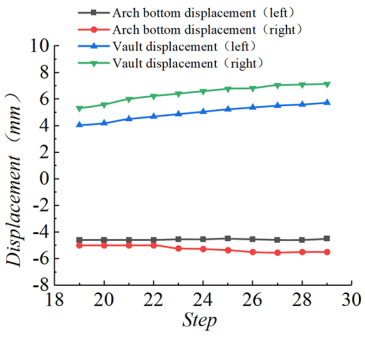

Figure 11. Displacement Diagram of Secondary Lining of Left and Right Tunnels

The secondary lining is built when the rock and soil are deformed and stabilized. The excavation of the tunnel has been completed before the secondary lining construction, so the displacement caused by it has not changed much, but each construction stage will influence each other. As shown in Figure 11, the displacement of the tunnel vault on the left (right) changes from 4.07mm (5.33mm) in the 19th step to 5.72mm (7.14mm) in the 29th step, an increase of about 40% (34%), and it is always 4.6mm (5.5mm) at the arch bottom. Both vault displacement and invert displacement are smaller in the left tunnel. It is concluded that for tunnel sections with different spans, under the premise that the deformation of the tunnel meets the requirements, the large-span tunnel has larger displacements.

V. Conclusion

This paper draws the following conclusions by simulating the construction process of the exit of the proposed Georgia No. 2 tunnel:

(1) Based on site parameters and rock physical and mechanical parameters, Midas GTS NX can simulate the redistribution of surrounding rock stress caused by tunnel excavation. However, the model cannot fully simulate the actual engineering geological conditions and stress field, and there will be certain errors. Therefore, it is necessary to build a more realistic model based on enough data to obtain better results and wider use.

(2) The pressure of surrounding rock has a great change before and after tunnel construction. After excavation is finished, the maximum value of the maximum principal stress is 105.5 times of the initial one, but the minimum has only increased by about 2 times. In the initial stage, the maximum and minimum values of the maximum principal stress appear at the surface and bottom of the rock and soil mass respectively. After excavation, the minimum value and maximum value appears in invert and waist section respectively, and their positions remain unchanged until the excavation is completed.

(3) After the construction of the tunnel entrance, the deformation at the top of the tunnel entrance shows a trend of gradual increase with the excavation. The deformation of tunnel entrance should be noticed during the actual construction.

(4) For the simultaneous construction of tunnels with different spans, the impact of the excavation of a large-span tunnel on the rock, soil, temporary lining, and the secondary lining is greater than the stress and deformation of the tunnel with a small span.

References

[1] Song, Z.P., Wang, T., Zhou, J.J., Yu, W.S. (2017) Analysis of Construction Optimization and Mechanical Characteristic of Shallow Large Section Tunnel. Chinese Journal of Underground Space and Engineering, 13: 459-468.

[2] Song, Z.P., Zhang, Q., Zhao, K.M., Zhang, X.G., Zhang, X.W., Wang, J.J. (2018) Optimization study on advance construction of double tunnel based on field monitoring and numerical analysis. Journal of Xi'an University of Architecture & Technology, 50: 654-661.

[3] Xu, Q.W., Cheng, P.P., Zhu, H.H., Ding, W.Q., Li, Y.H., Wang, W.T., Luo, Y. (2016) Model test and numerical simulation of progressive failure of surrounding rock across fault tunnel. Chinese Journal of Rock Mechanics and Engineering, 35: 433-445.

[4] Chen, L.H., Fu, H.L., Wang, H.T., Xu, C.D., Yu, L. (2017) Determination of Subsurface Excavation Method of Railway Tunnel Filled with Surrounding Rock Based on Numerical Simulation. Technological Development of Enterprise, 36: 1-5+28.

[5] Xing, J., Dong, X.B., He, X.N. (2018) Stability Analysis of Surrounding Rock in Tunnel Construction in Fault Fracture Zone. Journal of Catastrophology, 33: 164-168.

[6] Zhang, Z.L., Liu, Y.J., Guo, N.R. (2019) Deformation Analysis of Surrounding Rock for Large-span Shallow Buried Bias Tunnel. Subgrade Engineering, 4: 241-246.

[7] Guo, Z.H., Liu, X.R., Zhu, Z.Y. (2016) Limit equilibrium analysis of rock failure surface of shallow buried tunnel. Journal of Central South University, 47: 3217-3224.

[8] Guo, Z.H., Zhong, Z.L. (2017) Limit equilibrium analysis of fracture surface of shallow buried tunnel. Chinese Journal of Underground Space and Engineering, 13: 1228-1233.

[9] Liu, B., Zhang, D.W., Liu, S.Y., Qin, Y.J. (2017) Numerical simulation and field test of large section pipe jacking channel approaching through existing metro tunnel. Chinese Journal of Rock Mechanics and Engineering, 36: 2850-2860.

[10] Niu, Y.H., Tang, D.M. (2017) Analysis of Construction Method for Shallow Buried Tunnel Based on Numerical Simulation. Construction Technology, 46: 1126-1129.

[11] Li, K., Jia, C., Di, S.T., Zhang, J.P., Yu, Z.J. (2018) Monitoring Analysis on the Mechanical Properties for Tunnel Support System under Full Section Excavation. Chinese Journal of Underground Space and Engineering, 14: 860-868.